

Transient Response and Stability of the Bootstrap Variable Inductance (BVI)

Mohammad Tavakoli Bina
University of Surrey
tavakoli-bina@ieee.org

David C. Hamill
University of Surrey
d.hamill@surrey.ac.uk

Abstract — The Bootstrap Variable Inductance (BVI) is a new FACTS controller that emulates variable positive/negative inductance. Here, its stability and transient response is investigated in both shunt and series applications. For the series case, an IEEE benchmark is used. The BVI is shown to be inherently stable, and improves the power system stability in comparison with conventional capacitive compensation. Moreover, the risk of sub-synchronous resonance can be avoided.

I. Introduction

THE Bootstrap Variable Inductance (BVI) was first introduced in [4] and has been developed in [10]–[11] as a new FACTS controller. The BVI behaves as a variable positive/negative inductance emulator. It can be employed for series and parallel applications in ac power systems [4]. In [10]–[11], the basic concept of a negative inductance (*reductance*), and the PWM analysis of the BVI as a FACTS controller are discussed. In the present paper, the transient response and stability of the BVI are analysed. It is shown that the BVI improves the stability of power systems compared to the capacitive approach.

A. Overview of the BVI

Negative inductance was first proposed as a power-system series compensator in 1992, in the form of a “variable active-passive reactance” (VAPAR) [3], and this circuit has subsequently been developed by its inventors. In 1999, the BVI was presented for parallel and series applications in power systems. Fig. 1(b) shows a single-phase BVI circuit. An impedance Z connected to a variable gain amplifier $A(j\omega)$ provides a variable input impedance

$$Z' = \frac{V}{I} = \frac{Z}{1 - A(j\omega)} \quad (1)$$

where V and I are the input voltage and current phasors, respectively. Now suppose $A(j\omega) = A$ is a positive real constant. When $A < 1$, Z' has the same sign as Z but greater magnitude. When $A = 1$, $Z' = \infty$ so $I = 0$. When $A > 1$, Z' has the opposite sign to Z (negative impedance conversion). Thus if Z is an inductor ($Z = j\omega L$), the circuit will emulate a negative inductance, or *reductance*. The input reductance is $\Gamma' = -L'$, and the input impedance is $Z' = -j\omega\Gamma$. By

varying A , a wide range of inductance and reductance can be emulated, as shown in Fig. 1(a).

II. BVI's stability – shunted

Consider the autonomous system $\dot{\mathbf{x}} = \mathbf{f}(\mathbf{x})$. Then the equilibrium motion of $\mathbf{x}(t)$ is given a small disturbance. If the disturbed motion remains close to the unperturbed one $\mathbf{x}(t)$ for all time, then the autonomous system is stable. For small disturbances, the undisturbed motion is asymptotically stable if the effect on the motion tends to disappear. The motion is unstable if the effect tends to grow [8].

For a linear time-invariant system $\dot{\mathbf{x}}(t) = \mathbf{A}\mathbf{x}(t)$ to be stable, the eigenvalues of \mathbf{A} must be all lie in the left half plane. If all eigenvalues of \mathbf{A} have non-positive real part, then the system is stable. Eigenvalues with real part of zero produce undamped oscillation.

Considering Fig. 1(b), the BVI's state equations were derived, the copper losses $R = R_S$ being taken in series with the physical inductance L . With $\mathbf{x}(t) = [i_L, V_{C1}, -V_{C2}]^T$, the state equations are:

$$\dot{\mathbf{x}}(t) = \mathbf{A}(t)\mathbf{x}(t)$$

$$\text{where } \mathbf{A}(t) = \begin{bmatrix} -\frac{R}{L} & \frac{-1-s(t)}{2L} & \frac{-1+s(t)}{2L} \\ \frac{1+s(t)}{2C} & 0 & 0 \\ \frac{1-s(t)}{2C} & 0 & 0 \end{bmatrix} \quad (2)$$

This state equation represents a time-variant linear system. The only function of time is the switching function $s(t)$, which takes the values +1 and -1. If these values are substituted in $\lambda\mathbf{I} - \mathbf{A}$, we get:

$$\lambda\mathbf{I} - \mathbf{A} = \begin{bmatrix} \lambda + \frac{R}{L} & \frac{1}{L} & 0 \\ -\frac{1}{C} & \lambda & 0 \\ 0 & 0 & \lambda \end{bmatrix}_{s(t)=1} \quad (3)$$

$$\text{or } \lambda\mathbf{I} - \mathbf{A} = \begin{bmatrix} \lambda + \frac{R}{L} & 0 & \frac{1}{L} \\ 0 & \lambda & 0 \\ -\frac{1}{C} & 0 & \lambda \end{bmatrix}_{s(t)=-1}$$

These are now two time-invariant linear systems. The eigenvalues of \mathbf{A} are the roots of characteristic equation $\det(\lambda\mathbf{I} - \mathbf{A}) = 0$, or $\lambda(\lambda^2 + \frac{R}{L}\lambda + \frac{1}{LC}) = 0$. The eigenvalues of \mathbf{A} are:

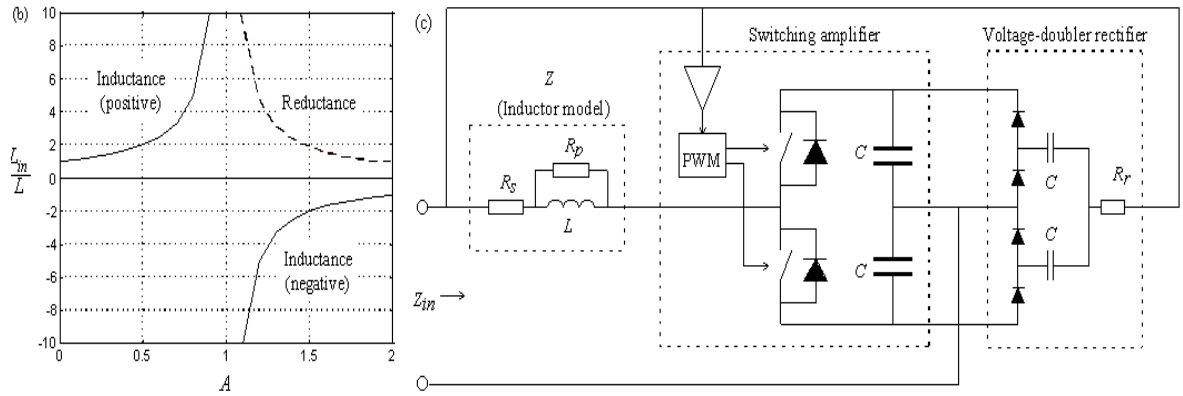


Figure 1: (a) range of emulated inductance L' as a function of amplifier gain A ; (b) BVI circuit schematic, showing a possible implementation with rectifier powering from the applied voltage.

$$\{\lambda\} = \left\{ \frac{-R - \sqrt{R^2 - 4Z_0^2}}{2L}, \frac{-R + \sqrt{R^2 - 4Z_0^2}}{2L}, 0 \right\} \quad (4)$$

where $Z_0 = \sqrt{L/C}$. One eigenvalue is zero because one of the capacitors is inactive at a given time. The other two eigenvalues are in the left-half plane, resulting in a stable system. They can be either complex ($R < 2Z_0$) or negative real ($R > 2Z_0$). If C is large — the usual case — we have two negative real eigenvalues, one near zero, the other close to $-R/L$. As $C \rightarrow \infty$, $Z_0 \rightarrow 0$ and the characteristic equation becomes $\lambda^2(\lambda + R/L) = 0$. The eigenvalues are now $\{\lambda\} = \{-R/L, 0, 0\}$ and the BVI acts like a first order element, with a time constant L/R . This result can also be obtained using the average circuit model of the BVI in [12].

If the eigenvalues are complex, however, we have a damped second-order system with a natural frequency $\omega_0 = 1/\sqrt{LC}$. This is undesirable for power systems use, and can usually be avoided by choosing C large enough. However, if this is not possible, the parameters should be chosen to avoid sub-synchronous resonance: the natural frequency should be placed outside the 15–30Hz range where mechanical resonances occur.

III. BVI's stability – series

Unlike the shunted case, the stability study is not straightforward for the series connected BVI. This is illustrated using the IEEE benchmark introduced in [1]. A BVI is inserted in series with the transmission line, as shown in Fig. 2. Here the BVI is represented by a reductance $\Gamma = L_B$ (assuming now that $R = 0$ and $C = \infty$).

Long transmission lines are best represented by distributed models, but the π -model and T-model can be used to a good approximation at 50/60Hz [6],[2],[9]. However, the frequency dependence of the line parameters and the distributed nature of the losses means that constant 50/60Hz values cannot adequately simulate the response of the line over the wide range of frequencies associated with transients.

Despite the drawbacks of a constant-parameter model, it is used in the present study because of its simplicity. The results

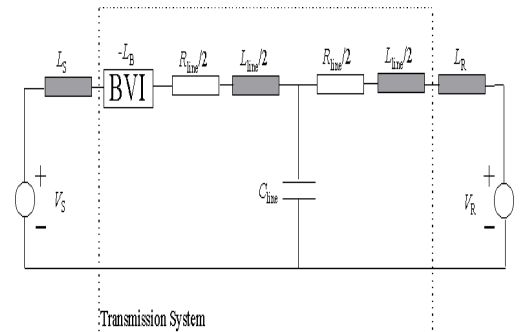


Figure 2: The benchmark T-model for stability analysis, suitable for the BVI installed at sending or receiving end.

of [6] indicate that the practical case will have more damping than predicted. The constant-parameter model therefore gives a pessimistic view, and practical stability should be better than predicted.

A. Stability – T-model

Fig. 2 introduces the T-model which is useful for studying a series compensator installed at one end of the line. The state space equation is:

$$\begin{aligned} \dot{\mathbf{x}}(t) &= \mathbf{A}\mathbf{x}(t) + \mathbf{b}\mathbf{u}(t) \\ \mathbf{A} &= \begin{bmatrix} \frac{-R_{line}}{2(L_{line}/2 - \Gamma + L_S)} & 0 & \frac{-1}{L_{line}/2 - \Gamma + L_S} \\ 0 & \frac{-R_{line}}{2(L_{line}/2 + L_R)} & \frac{1}{L_{line}/2 + L_R} \\ \frac{1}{C_{line}} & \frac{-1}{C_{line}} & 0 \end{bmatrix} \\ \mathbf{b} &= \begin{bmatrix} \frac{1}{L_{line}/2 - \Gamma + L_S} & 0 \\ 0 & \frac{1}{L_{line}/2 + L_R} \\ 0 & 0 \end{bmatrix} \\ \mathbf{x}(t) &= [i_S \quad i_R \quad V_{C_{line}}]^T, \mathbf{u}(t) = [V_S \quad V_R]^T \end{aligned} \quad (5)$$

where R_{line} , C_{line} , L_{line} are the transmission line lumped parameters, Γ is the variable reductance of the BVI, V_S , L_S , are the sending-end parameters, and V_R , L_R are the

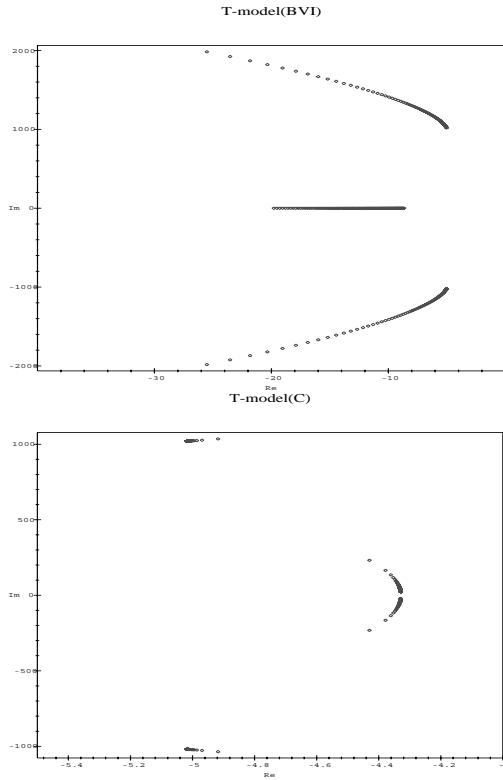


Figure 3: Root locus for the IEEE benchmark under series compensation using (a) the BVI installed at one end, and (b) a capacitor bank installed at one end.

receiving-end parameters. These parameters for the IEEE benchmark [1] are as follows: $R_{line} = 0.02\Omega$, $L_{line} = 1.3\text{mH}$, $C_{line} = 1.8\text{mF}$, $L_S = 0.8196\text{mH}$, $L_R = 0.191\text{mH}$. The reference voltage V_R has a magnitude of 1.0p.u.

The characteristic equation can be obtained using $\det(s\mathbf{I} - \mathbf{A}) = 0$, or from the system's transfer functions (e.g. I_S/V_R). Using either approach, we find:

$$(-1.47 \times 10^{-3} + \Gamma)s^3 + (-2.75 \times 10^{-2} + 11.89\Gamma)s^2 + (-1526.51 + 660589.24\Gamma)s - 13211.78 = 0 \quad (6)$$

The BVI's reactance Γ is the parameter of (6). It can be varied over say $[0, L_{line}]$, i.e. 0% to 100% series compensation. In practice, the series compensation does not exceed 80% [7].

To assess the the stability, it is necessary to find the roots of (6) for different values of Γ . A program was written to solve (6) and the solutions are plotted in Fig. 3(a) as a root-locus for variable series compensation.

For comparison, the BVI was replaced with a capacitance C_B . The characteristic equation is now

$$C_B s^4 + 18.69C_B s^3 + (1038689.11C_B + 680.43)s^2 + (8989749.20C_B + 8090.77)s + 449487460.0 = 0 \quad (7)$$

The capacitance C_B is the parameter of (7). This can be varied to provide 0% to 100% series compensation, like Γ in

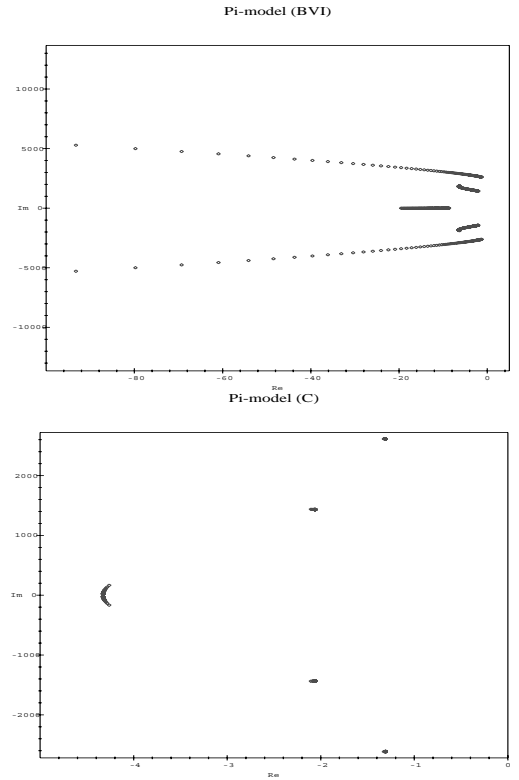


Figure 4: Root locus for the IEEE benchmark under series compensation using (a) the BVI installed at the middle of the line, and (b) a capacitor bank installed at the middle of the line.

Table 1: BVI's and capacitor's root-locus summary (T-model): $\Gamma \in [0, 1.3]\text{mH}$ and $C_B \omega_s \in [0.01, 0.41]\Omega$

	Eigenvalues (rad/s)	Damping ratio ($\frac{-Re(\lambda)}{Im(\lambda)}$)	Compensator
From	$-8.65 \pm j0$	∞	BVI
	$-4.32 \pm j23.16$	0.1834	C
To	$-19.80 \pm j0$	∞	BVI
	$-4.42 \pm j231.80$	0.0191	C
From	$-5.02 \pm j1019$	0.0049	BVI
	$-5.02 \pm j1019.26$	0.0049	C
To	$-25.50 \pm j1983.50$	0.0129	BVI
	$-4.91 \pm j1035.40$	0.0047	C

(6). Fig. 3(b) shows the root-locus of (5). The results are summarised in Table 1 for comparison and assessment.

There are some points for discussion regarding Figs. 3(a) and (b). First, over $[0\%, 100\%]$ series compensation, both the BVI and capacitor give a stable system. With the BVI we have one negative real and two complex eigenvalues, whereas with capacitive compensation we have four complex eigenvalues (see Table 1).

Second, as a measure of stability, the damping ratios (defined as $-Re(\lambda)/Im(\lambda)$) can be compared. For the BVI's complex poles, the damping ratio increases from 0.0049 to 0.0129. For the capacitor case, the corresponding eigenvalues have a damping ratio decreasing from 0.0049 to 0.0047. The reductive compensation is more highly damped than capacitive compensation. The BVI has an additional negative real eigenvalue, whereas the capacitor case has two more complex eigenvalues with a decreasing damping ratio from 0.1834 to 0.0191.

Third, sub-synchronous resonance (SSR) [5] occurs typic-

ally at 15–30Hz. The capacitor case has natural frequencies in the range 3–37Hz, overlapping the SSR frequency range. The BVI, however, introduces no risk of SSR, an advantage over capacitive compensation.

B. Stability – π -model

Fig. 5 introduces the π -model, which is useful for studying a series compensator installed at the middle of the line.

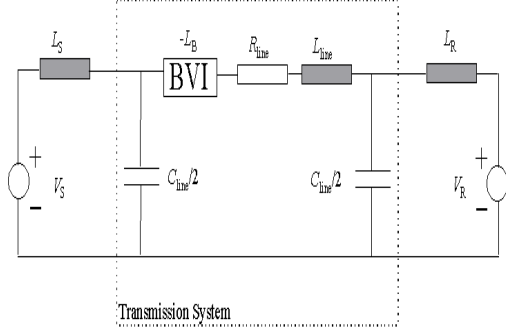


Figure 5: The benchmark π -model, suitable for the BVI installed at the middle of the line.

As for the T-model, the state space equation of the π -model and BVI leads to a characteristic equation:

$$(1.69 \times 10^{-6} - 0.0026\Gamma + \Gamma^2)s^5 + (2.60 \times 10^{-5} - 0.02\Gamma)s^4 + (15.01 - 20871.83\Gamma + 7.17 \times 10^6\Gamma^2)s^3 + (186.49 - 143458.56\Gamma)s^2 + (2.37 \times 10^7 - 2.85 \times 10^{10}\Gamma + 7.89 \times 10^{12}\Gamma^2)s + (2.05 \times 10^8 - 1.58 \times 10^{11}\Gamma) = 0 \quad (8)$$

As before, the root-locus of (8) is plotted in Fig. 4(a), by varying Γ over $[0, L_{line}]$. Again, the BVI was replaced with a capacitance C_B , leading to the characteristic equation:

$$C_B s^6 + 15.38C_B s^5 + (8882329.52C_B + 769.23)s^4 + (110352735.6C_B)s^3 + (1.40 \times 10^{13}C_B + 5517636781)s^2 + (1.21 \times 10^{14}C_B)s + 6.07 \times 15 = 0 \quad (9)$$

The capacitance C_B is varied to provide 0% to 100% series compensation, and Fig. 5(b) shows the root locus. Table 2 summarises the results for comparison.

Table 2: BVI's and capacitor's root-locus summary (π -model): $\Gamma \in [0, 1.3]mH$ and $C_B\omega_s \in [0.01, 0.41]\Omega$

	Eigenvalues (rad/s)	Damping ratio ($\frac{-Re(\lambda)}{Im(\lambda)}$)	Compensator
From	$-8.65 \pm j0$	∞	BVI
To	$-4.32 \pm j23.16$	0.1834	C
From	$-19.54 \pm j0$	∞	BVI
To	$-4.26 \pm j165.89$	0.026	C
From	$-2.06 \pm j1432.5$	0.0014	BVI
To	$-2.05 \pm j1432.16$	0.0014	C
From	$-6.29 \pm j1886$	0.0033	BVI
To	$-2.10 \pm j1437.17$	0.0015	C
From	$-1.30 \pm j2613.45$	0.0005	BVI
To	$-1.30 \pm j2613.48$	0.0005	C
From	$-93.26 \pm j5286.92$	0.0176	BVI
To	$-1.3 \pm j2615.06$	0.0005	C

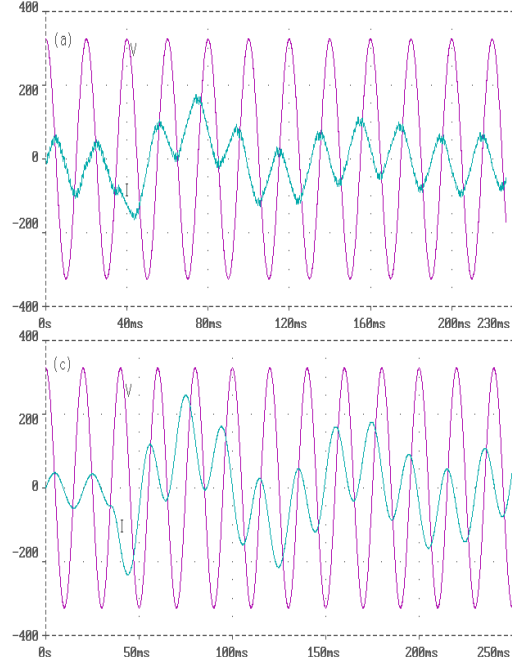


Figure 6: Simulation results of BVI's transient taken from (a) exact BVI, and (b) the average model (amplifier's gain changes from $A = 0.5$ to $A = 2$ at $t = 35ms$).

The BVI case has one negative real and four complex eigenvalues, while the capacitor case has six complex eigenvalues.

As with the T-model, Table 2, shows that the damping ratio is improved by using the BVI, and SSR is avoided with the BVI, whereas it is a possibility with capacitance. Both models indicate stability improvement by employing a BVI in place of the conventional capacitor bank for series compensation.

IV. BVI's transient response

Next, the BVI's transient response for shunt and series applications is investigated. The shunt connected BVI is subjected to sudden changes in the amplifier gain and the input voltage. The IEEE benchmark and the average model of the BVI are used for transients in the series case.

A. Shunted case

Steady state simulations in [12] showed that the average model provides a good approximation for the BVI. Here we show that it is also a good model for transients. Simulations using the average model are compared with ones using the exact (switching) BVI circuit.

Fig. 1 is considered for simulation of the exact BVI, along with the following parameters: nominal shunt voltage 230V 50Hz, physical inductance 12mH, copper loss resistance 0.15 Ω , iron loss resistance 500k Ω , amplifier capacitance 8.1mF, and voltage doubler capacitance 8.1mF. The amplifier gain and the applied voltage can be varied. The initial conditions for the capacitor voltages were $\pm 640V$.

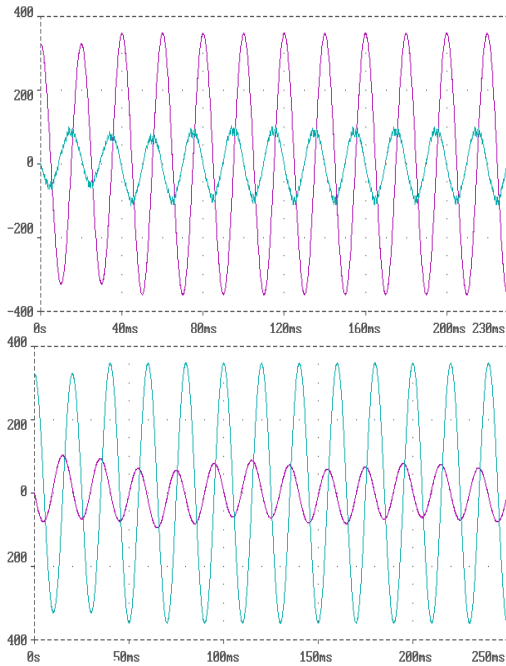


Figure 7: Simulation results of BVI's transient taken from (a) exact BVI, and (b) the average model (applied voltage changes from 230V to 250V at $t = 35\text{ms}$).

In the first simulation, the gain was initially set to $A = 0.5$ (inductance emulation). At $t = 35\text{ms}$, A is suddenly changed to 2.0 (reductance emulation). This instant gives the worst case because the BVI's current is at its peak, and consequently the current increases to twice the normal peak value.

Fig. 6(a) shows the simulation results of the average model, while Fig. 6(b) depicts the exact simulation results. The simulations agree well with each other, except that the average model has no switching ripple. Immediately after $t = 35\text{ms}$, the current starts leading the voltage. Thus the BVI is emulating reductance throughout the transient.

B. Series case

The IEEE benchmark is used for series simulations. Although the BVI's input voltage can change, A should remain constant so the emulated impedance does not vary. Therefore, the PWM modulation index must vary during a transient in order to keep the amplifier's gain fixed.

Two simulations are considered. First, a transient was produced by changing the mechanical power of the generator. The electrical power transmitted through the transmission line is proportional to the phase difference δ between the generator emf and the receiving-end voltage. The stability of the generator can be examined by observing $\delta(t)$. If δ exceeds a critical angle, then the motion of the rotor is out of control. If δ increases without limit, the generator loses its synchronism and becomes unstable.

A simulation was performed with SIMULINK. The generator was modelled and its mechanical power was changed from 0.3p.u. to 0.4p.u. The voltage divider was set for a

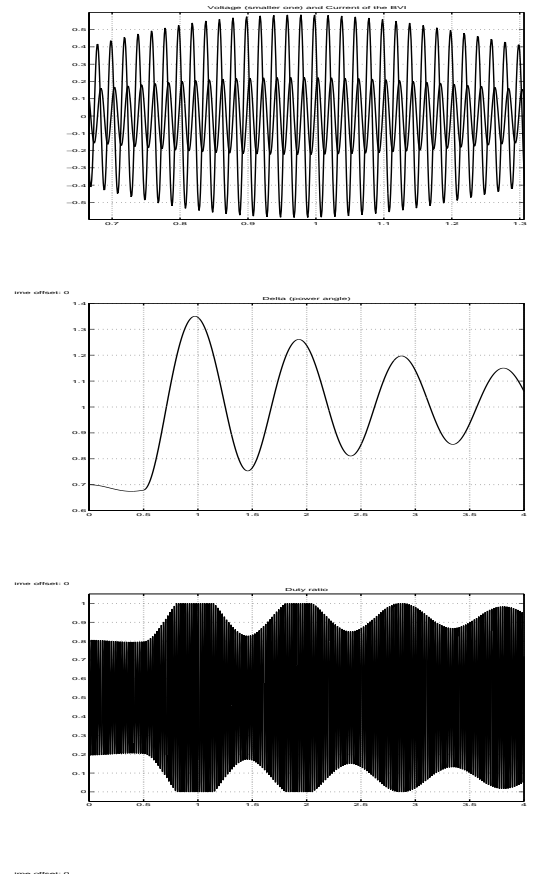


Figure 8: Simulation results of the BVI's transient under series compensation (a) the BVI's voltage and current, (b) the power angle δ , and (c) the duty ratio of the switching amplifier.

gain of $A = 1.50$. The amplifier's duty ratio was limited to the range $[0, 1]$, as in practice. The electrical part of the benchmark, including the BVI, was modelled using state-space equations. The results are presented in Fig. 8(a)–(c). Fig. 8(a) shows the BVI's current and input voltage. The voltage and current both change proportionately, so the BVI properly emulates a fixed impedance.

The variation of δ is shown in Fig. 8(b). The power angle δ slowly approaches its steady state, via a slowly damped oscillation at about 1Hz. This is a stable case. (Without a compensator, the system would be unstable.) Fig. 8(c) illustrates the variation of the PWM reference during the transient.

In the second set of simulations, the BVI provides a transient itself as the amplifier's gain is changed. Two cases were considered. First, the amplifier's gain was changed from $A = 1.5$ to $A = 1.9$ at $t = 0.5\text{s}$, followed by another change to $A = 1.3$ at $t = 0.8\text{s}$ (Fig. 9, top right-hand picture). This is reductive compensation throughout. Second, the gain was changed from $A = 1.6$ to $A = 0.5$ at $t = 0.5\text{s}$, then to $A = 1.9$ at $t = 0.8\text{s}$ (Fig. 9, bottom right-hand picture). This is reductive, then inductive, then back to reductive.

The top and bottom left-hand pictures in Fig. 9 show the input voltage and current of the BVI. In both cases, the power system current increases or decreases quite smoothly.

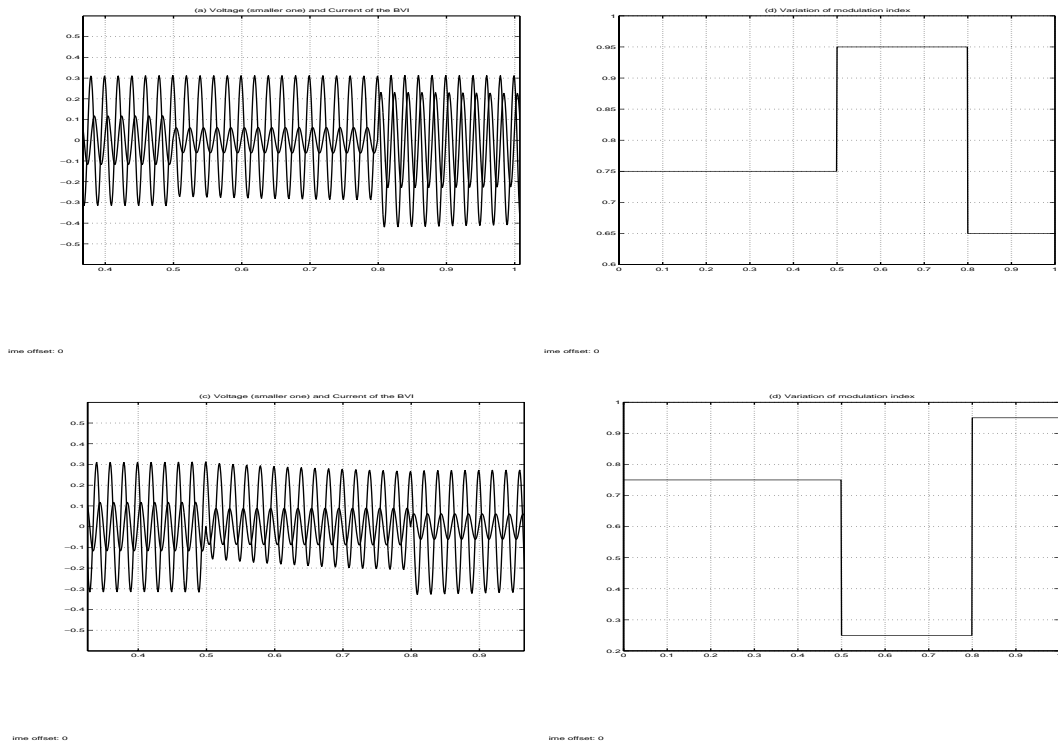


Figure 9: Simulation results of the BVI's transient under series compensation (a), (c) are the BVI's voltage and current under variation in modulation index shown in (b) and (d) respectively.

V. Conclusion

We have shown by simulations that the BVI improves power system stability in comparison with the conventional capacitive approach. Furthermore, the BVI's transient response has been examined for the series and shunted cases, and is satisfactory. The simulations show that the BVI can be used in place of capacitive compensation, giving improved stability and flexibility.

References

- [1] IEEE Task Force of the Dynamic System Performance Working Group. Benchmark. First benchmark model for computer simulation of subsynchronous resonance. *IEEE Transactions on Power Apparatus and Systems*, PAS-96(5):1565–1572, September 1977.
- [2] A. Budner. Introduction of frequency-dependent line parameters into an electromagnetic transient program. *IEEE Transactions on Power Apparatus and Systems*, PAS-89(1):88–97, January 1970.
- [3] A. Funato and A. Kawamura. Realisation of negative inductance using variable active-passive reactance (vapar). *IEEE Transactions on Power Electronics*, 12(4):589–596, July 1997.
- [4] D. C. Hamill and M. Tavakoli-Bina. The bootstrap variable inductance and its applications in ac power systems. In *IEEE Applied Power Electronics Conference (APEC)*, volume 2, pages 896–902, March 1999.
- [5] P. Kundur. *Power system stability and control*. McGraw-Hill, 1993.
- [6] J. R. Marti. Accurate modelling of frequency-dependent transmission lines in electromagnetic transient simulation. *IEEE Transactions on Power Apparatus and Systems*, PAS-101(1):147–157, January 1982.
- [7] T. J. E. Miller. *Reactive power control in electric systems*. Wiley, 1982.
- [8] P. W. Sauer and M. A. Pai. *Power system dynamics and stability*. Prentice Hall, 1998.
- [9] J. K. Snelson. Propagation of travelling waves on transmission lines frequency-dependent parameters. *IEEE Transactions on Power Apparatus and Systems*, PAS-91(1):85–91, January/February 1982.
- [10] M. Tavakoli-Bina and D. C. Hamill. The bootstrap variable inductance: a new facts control element. In *IEEE Power Electronics Specialists Conference (PESC)*, volume 2, pages 619–625, June 1999.
- [11] M. Tavakoli-Bina and D. C. Hamill. Harmonic analysis of the pwm series/parallel bootstrap variable inductance. In *IEEE Power Electronics and Drive Systems (PEDS)*, volume 1, pages 22–27, July 1999.
- [12] M. Tavakoli-Bina and D. C. Hamill. The averaged model of the bootstrap variable inductance (bvi). In *IEEE Power Electronics Specialists Conference (PESC)*, volume 2, pages 967–972, June 2000.